Ceramics International **21** (1995) 69–75

Microchemistry and Microstructure of Some Opaque Glaze/Tile Interfaces in Relation to their Physical Properties

S. A. El-Defrawi,[a] M. A. Serry,[a] W. I. Abd El-Fattah[a] & W. Weisweiler[b]

[a] Ceramic Department, National Research Centre, Dokki, Cairo, Egypt
[b] Institute of Chemical Technology, University of Karlsruhe, Karlsruhe, Germany

(Received 26 June 1993; accepted 24 February 1994)

Abstract: Physical properties of some double- and once-fired glazed tiles were assessed in the light of the microchemistry and microstructure of their interfaces as investigated using a computer-controlled electron-probe microanalyzer. The properties investigated are melting temperatures and thermal expansion of glazes, as well as crazing resistance and gloss of glaze surfaces. The double- and once-fired glaze layers are strongly bound to their ceramic tiles, as indicated by high resistance to crazing. The application of zircon-ZnO opacifying mixtures in the presence of 5·0–8·0 wt% B_2O_3 leads to maximizing the gloss of glaze surfaces. Increasing B_2O_3 content enhances bubble formation whereas a mat layer results at the surface of once-fired glazes containing higher zircon and ZnO contents at the expense of B_2O_3. The recrystallization of silicate phases, especially in double-fired glazes, is hindered by minimizing the lime and alkali oxides content in the presence of up to 10wt% ZnO.

1 INTRODUCTION

The application of the electron-probe microanalyzer (EPMA) for investigating glaze/ceramic interfaces is a useful tool to simultaneously study the microchemistry and microstructure of glaze, interaction zone and ceramic body. Hence, physical properties of glazed-ceramic bodies, e.g. gloss, resistance to crazing and thermal expansion, can actually be assessed in the light of EPMA investigations.[1,2] Opaque glazed tiles are produced using once- and double-fired techniques. The glaze surface characteristics of both types depend not only on glaze itself but also upon the nature of the body and its interaction during firing. The interfacial layer of the body dissolved in the glaze allows glaze to withstand thermal shocks more readily. Proper interaction depends upon the firing process and the total composition of the glaze, as well as its individual compounds.

All glazed tiles presumably contain some bubbles in their glaze and interfacial layers which, if sufficiently numerous, can influence their properties.[2–5]

The coverage capacity and wetting characteristics of a glaze are controlled by its surface tension, contact angle, viscosity and opacity.[6] Opaque glazes should have a considerable amount of finely dispersed opacifying material exhibiting a noticeable difference in refractive index with the glassy matrix. Zircon ($ZrSiO_4$), ZrO_2, ZnO, TiO_2 and SnO_2 are used as opacifying agents to produce opaque glazes. $ZrSiO_4$ was proved to enhance opacity, especially in the presence of ZnO providing that SiO_2/Al_2O_3 molar ratio is equal to 10.[3–6]

In a previous work,[7,8] the properties of semi-industrially prepared double- and once-fired glazed tiles were investigated and some of them were selected on the basis of their composition and properties. The aim of the present work is to study the microchemistry and microstructure of the interfaces of these tiles using EPMA in relation to their properties: namely gloss, thermal expansion and crazing resistance.

Ceramics International 0272-8842/95/$9.50

2 EXPERIMENTAL PROCEDURE

2.1 Preparation of glaze slips

Three frit formulae were designed, thoroughly mixed and fused at approximately 1300°C in a pilot gas furnace for 4 h. The mature melts were quenched in tap-water and the produced frits were used for the preparation of both engobe and glaze slips. The engobe slips were prepared by wet-milling of 1/1 weight ratio of frit plastic kaolin mixtures with 45wt% water. These slips were applied on the surface of 15×15 cm green and fired tiles as an intermediate layer between glaze and body to prepare once- and double-fired glazed tiles, respectively. For double-fired glazes, 5wt% plastic kaolin and 0·3wt% carboxy methyl cellulose (CMC) were added to 100wt% of the prepared frit. In the case of once-fired glazes, mixtures of 65wt% frit, 15wt% plastic kaolin, 2wt% Al_2O_3, 0·3 wt% CMC as well as various ratios of $ZrSiO_4$ and ZnO were added, up to 100%. For both types of glazes, 45wt% of tap-water was added, wet-milled for 5 h to prepare slips of density 1750 g/litre and 1650 g/litre for the production of double- and once-fired tiles, respectively. The glazed biscuit and green tile samples were fired in an industrial tunnel kiln using the nominal firing-schedules of 18 h or 55 min to produce double- and once-fired tiles, respectively. The maximum temperatures of these schedules were 980 and 1080°C, respectively.

2.2 Assessment of glazed tiles

The microchemistry and microstructure of the glaze/tile interfaces were studied after slicing, embedding in polymer resin, gradual polishing and coating with a carbon thin film of 1×1 cm samples. A computer-controlled microanalyzer of the type CAMEBAX SX 50 attached with an energy dispersive system (EDS) for tracing light elements was used for this investigation. The microstructure was revealed from back-scattered electron images (BSE) whereas line scans were carried out across glaze, interface and ceramic body to follow up the minor variations of oxide contents at 10 μm intervals by stepwise point analysis.

The phase composition, as well as physical properties, of glaze and its surface were investigated. X-ray diffraction (XRD) was used for the qualitative determination of crystalline phases of frit and glaze samples. Melting temperatures of glaze compositions were followed in the range of 900–1050°C applying the cone fusion test.[3,4] The thermal expansion coefficient (α) of glaze samples was calculated at 580°C from the thermal expansion curves obtained using an automatic THETA dilatometer according to ANSI/ASTM procedure C8 24-76. Specular gloss of glaze surfaces was measured at 60° using a glossmeter of the type D 48 D (ANSI/ASTM C 58-71). The resistance of glaze surfaces to crazing was evaluated after steam-curing in an autoclave according to ANSI/ASTM C 424-60. Ten identical uncut glazed tiles were steam-cured at a pressure of 3·5 kg/cm^2 and gradually increased up to 17·5 kg/cm^2 at intervals of 3·5 kg/cm^2. A dye solution was used for the examination of glaze surfaces after each test.

3 RESULTS AND DISCUSSION

Table 1 illustrates the chemical composition of the ceramic body, as well as glaze formulations used for double- and once-fired glazed tile samples. The double-fired samples are referred to as DF1, DF2 and DF3, whereas OF1, OF2 and OF3 represent the once-fired species. It is evident that the body is mainly composed of $SiO_2{\cdot}Al_2O_3{\cdot}CaO$ and Fe_2O_3 in addition to limited amounts of TiO_2, MgO, Na_2O

Table 1. Chemical composition of the ceramic body and glazes used for double- and once-fired ceramic tiles

Oxide weight %	Body (biscuit)	Double-fired glaze DF1	DF2	DF3	Once-fired glaze OF1	OF2	OF3
SiO_2	60·96	55·93	56·23	58·31	48·47	48·63	52·23
Al_2O_3	22·78	3·85	9·20	8·89	9·46	13·20	12·05
Fe_2O_3	1·94	—	—	—	—	—	—
TiO_2	1·19	—	—	—	—	—	—
B_2O_3	—	5·98	13·30	8·19	4·18	9·36	6·22
ZrO	—	6·97	7·60	7·70	12·79	13·22	8·51
ZnO	—	9·97	1·90	5·28	13·10	7·46	12·25
CaO	10·92	10·98	1·93	3·87	7·66	1·33	2·95
MgO	0·61	2·22	0·97	0·69	1·40	0·67	0·51
Na_2O	0·71	4·05	8·61	3·70	2·79	5·98	2·76
K_2O	0·89	0·05	0·05	3·36	0·15	0·15	2·52
Acid/base ratio	—	2·05	4·18	3·45	1·93	3·12	2·49

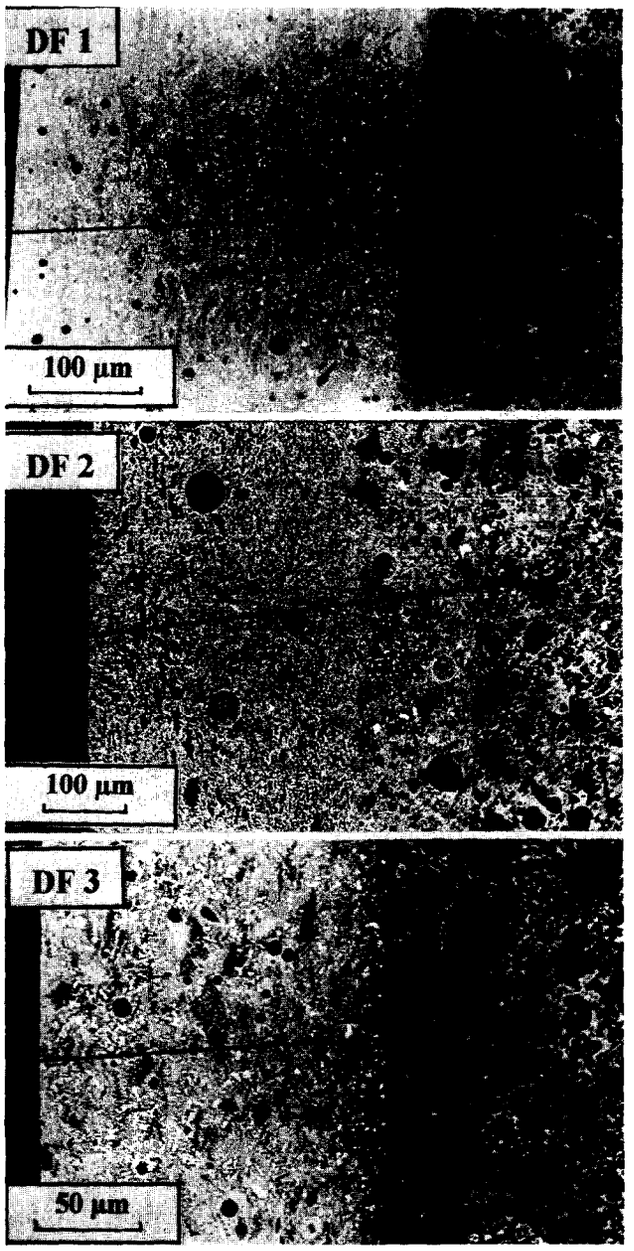

Fig. 1. Back-scattered electron images (BSE) of double-fired glazed tile samples.

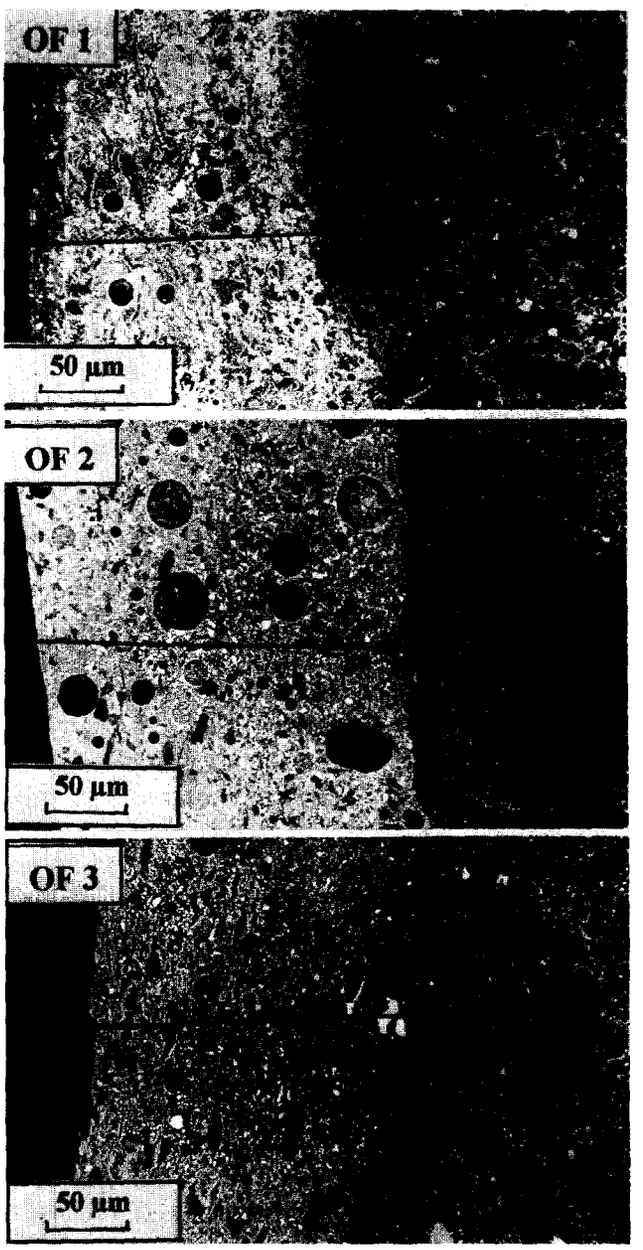

Fig. 2. Back-scattered electron images (BSE) of once-fired glazed tile samples.

and K_2O. Therefore, on firing this body up to 1100°C, anorthite ($CaO{\cdot}Al_2O_3{\cdot}2\ SiO_2$), free quartz and glassy phase are the main phases, as previously detected in its biscuit by XRD.[7,8]

Concerning the glaze compositions, SiO_2 is the major oxide. Its content ranges between 55 and 59wt% for double-fired samples, while once-fired glazes contain a lower level (48–53wt%). The latter samples also show lower Al_2O_3 content (3–9 wt%) as compared with double-fired ones (9–14 wt%). The acid/base ratio $SiO_2/(R_2O + RO)$ for all samples ranges between 1·93 and 4·18. The lower acid/base ratio of DF1 and OF1 glazes can be attributed to their much higher content of ZnO, CaO and/or Na_2O. The latter oxide is the main alkali oxide present in all samples except in DF3 and OF3 which contain a mixture of approximately equal amounts of Na_2O and K_2O.

Figures 1 and 2 exhibit the back-scattered electron images (BSE) obtained by EPMA investigations of glaze/tile interfaces of all samples. The line scans done to follow-up variations of chemical composition across these interfaces are superimposed on the BSE images, the length of which varies between 210 and 490 μm. Generally, as the thickness of the glaze layer increases in double-fired samples, longer line scans are obtained.

The calculated mean values of chemical composition of glaze, interface and ceramic body as determined by stepwise point analysis along each line scan are summarized in Tables 2 and 3. It is worth noting here that B_2O_3 cannot be quantitatively detected, but it is qualitatively traced for

Table 2. Computerized mean chemical composition of interface layers of the double-fired glazed tile samples as determined by microprobe analyzer

Layer	DF1			DF2			DF3		
	Glaze	Interface	Body	Glaze	Interface	Body	Glaze	Interface	Body
SiO_2	46·98	52·74	47·69	58·03	63·81	57·69	55·59	61·55	53·95
Al_2O_3	13·43	22·67	14·47	11·48	14·95	18·08	9·88	12·72	22·05
FeO	0·24	0·75	2·63	0·19	0·83	4·51	0·28	0·45	1·12
TiO_2	0·20	0·50	0·72	0·21	0·70	2·74	0·08	0·21	0·55
ZrO_2	10·04	1·82	0·18	7·00	3·86	0·02	7·37	6·18	0·43
ZnO	9·44	3·07	0·17	1·81	2·11	0·18	10·54	4·04	1·42
CaO	2·55	2·22	8·83	3·72	2·44	8·96	3·65	2·71	3·90
MgO	0·07	0·19	0·23	0·10	0·14	0·40	0·61	0·44	0·35
Na_2O	4·84	3·30	1·02	5·42	4·84	2·23	3·16	3·04	2·08
K_2O	0·40	0·93	0·28	0·84	0·80	0·25	2·12	2·44	1·62
Total	88·19	98·11	76·22	88·80	94·48	95·06	93·28	93·78	87·47

sample DF1 as an example (Fig. 3). The total oxide contents are lower than 100% in glaze, and the interfacial layer is mainly due to the undetermined B_2O_3, while in case of the ceramic body it is related to its porous microstructure.

The microstructure of the ceramic body as shown in Figs 1 and 2 exhibits pores with variable sizes and shapes (black) in between quartz grains (dark grey), anorthite patches (light grey) and fine iron-oxide rich crystals (very bright). All of these phases are bonded by a glassy phase (bright).

The interfacial layer of all samples can easily be distinguished in Figs 1 and 2 according to its intermediate brightness as a reaction product between the opacified glaze and the darker ceramic body. Also, an abrupt decrease in ZnO and ZrO_2 concentrations is observed towards the body at the contact of intermediate layer with glaze and body which contains traces of these oxides (Tables 2 and 3). In all samples, the interfacial layer exhibits quartz grains of variable sizes embedded in ZnO- and ZrO_2-rich bright silicate matrix. It is evident that more regular interaction layers are observed in double-fired samples as compared with those of once-fired specimens. This is mainly attributed to the more vigorous attack of glaze on green tiles in the case of the latter samples which are also fired at a relatively high temperature of 1080°C.[3,4]

Both the glaze and interfacial layers of all samples show round, closed pores (bubbles) of variable number and size. The formation of such bubbles is mainly due to the liberation of some gases from the ceramic body and/or glaze during glaze melting at later stages.[3,4] In the early stages of cooling, most of the gases entrapped in the bubbles contract and draw the glaze surface downwards, leading to the formation of pin-holes and pits.[9,10] The formation of such surface defects is evident in samples DF2, OF2 and OF3 (Figs 1 and 2). The relative increase of bubble size in samples DF2 and OF2 is related to its higher content of B_2O_3 (9–14wt%) as severe flux and also to its higher acid/base ratio (3·0–4·2), i.e. higher viscosity during melting. The larger pore size in sample OF2 is attributed to the faster rate and higher temperature of its melting during the once-firing process as compared with the conventionally fired DF2 sample (11–13).

Table 3. Computerized mean chemical composition of interface layers of the once-fired glazed tile samples as determined by microprobe analyzer

Layer	DF1			DF2			DF3		
	Glaze	Interface	Body	Glaze	Interface	Body	Glaze	Interface	Body
SiO_2	50·79	60·32	51·99	46·51	51·83	45·30	57·74	48·68	43·87
Al_2O_3	13·27	16·37	13·96	14·10	18·96	24·65	8·79	14·71	20·13
FeO	0·27	0·86	3·03	0·29	0·48	2·66	0·28	3·38	2·63
TiO_2	0·25	0·83	2·16	0·12	0·20	1·01	0·15	5·08	0·74
ZrO_2	13·73	4·17	0·08	12·72	7·73	0·19	7·32	4·93	0·03
ZnO	6·72	1·92	0·10	10·06	5·76	0·74	5·01	2·46	0·21
CaO	2·59	1·69	12·56	8·08	5·90	8·72	5·24	2·38	10·59
MgO	0·13	0·43	0·25	0·14	0·21	0·42	0·24	0·21	0·24
Na_2O	4·31	1·18	0·88	2·20	2·61	2·81	3·76	2·78	1·48
K_2O	0·59	0·82	0·14	0·59	1·42	1·19	2·12	1·59	0·28
Total	92·65	94·59	85·15	94·81	95·10	87·67	90·65	86·20	80·19

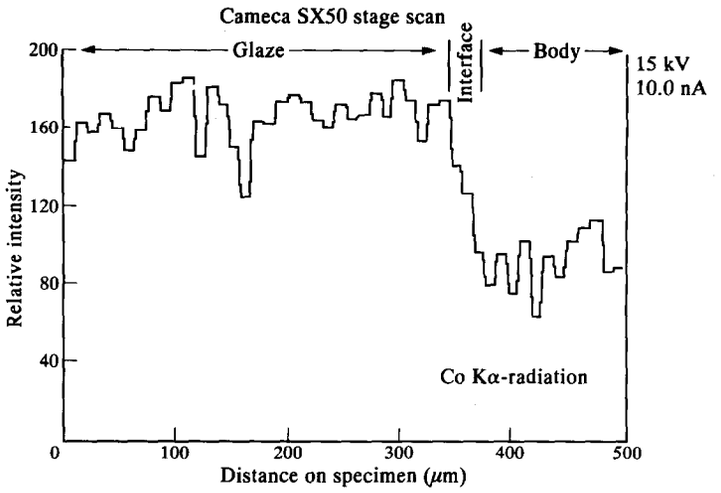

Fig. 3. Tracing of boron across the glazes, interface and ceramic body for DF1 glazed tile samples.

The glaze layer of all samples show that bright zircon grains with variable sizes are the main opacifying agents. In sample DF2 (Fig. 2), the size of zircon grains is reduced to less than 1 μm and dessiminated in the glassy silicate matrix (grey) as detected by focussing the electron beam at higher magnification. The presence of very high B_2O_3 content in DF2 (13–30 wt%) minimizes the size of zircon grains by dissolution in B_2O_3-rich glassy phase. This is responsible for the brightness of the DF2 glaze in spite of its lower ZnO content (1·9 wt%). The addition of higher amounts of ZnO (5–13 wt%), together with zircon in the rest of glazes, increases its brightness due to enrichment of the glassy silicate matrix by ZnO as shown in Figs 1 and 2. In samples DF2 and OF3, some coarse zircon grains are also embedded in its interfacial layer. Zircon is known to be the major crystalline phase, promoting opacity in zirconium glazes regardless of the type of zirconium-bearing opacifier used.[14]

Figure 4 shows the XRD patterns of DF1 and OF1 glaze samples. Some silicate phases, namely anorthitic plagioclase s.s. $\{(Na, Ca)\cdot AlSi_3O_8\}$, as well as ($Na_2O$, ZnO)-zirconium alumino silicate s.s. phases, are detected beside zircon, the main crystalline phase detected in all glaze samples. In glaze DF1, the (Na_2O, ZnO)-zirconium alumino silicate s.s. predominates at the expense of zircon and plagioclase s.s. phases. The chemical analysis of the former phase is determined by point analysis along line scanning of DF1 and OF1 glazes; its mean values are given in Table 4. As shown in Table 1, the strong increase of CaO (7–11 wt%) in these glazes together with higher ZnO (9–13 wt%) and Na_2O (6–8·6 wt%) contents lead to a decrease in its acid/base ratio down to 1·9–2·1 wt%, which in turn enhances the glaze fluidity during melting up to 980 and 1080°C, respectively. Hence, the ionic diffusion accelerates in the glaze melts and the above silicate phases recrystallize during cooling. If the amount of lime is increased

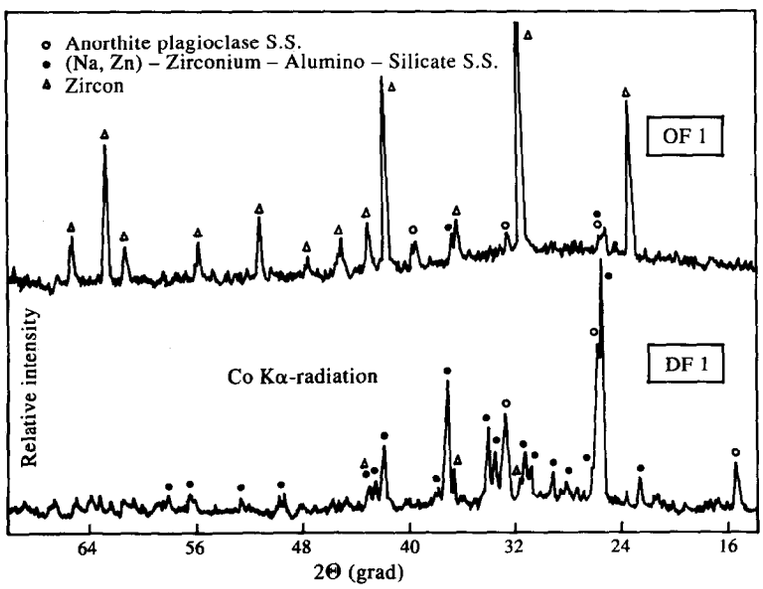

Fig. 4. XRD patterns of DF1 and OF1 glaze samples.

Table 4. Mean chemical composition of the Na_2O, ZnO–zirconium–alumino–silicate phases as detected by point analysis in samples DF1 and OF1

Oxide	DF1	OF1
SiO_2	40·96	46·26
Al_2O_3	18·24	15·15
FeO	0·30	0·35
TiO_2	0·26	0·33
ZrO_2	9·40	15·83
ZnO	12·69	9·27
CaO	2·34	2·29
MgO	0·07	0·13
Na_2O	4·74	3·86
K_2O	0·35	0·52
Total	89·35	93·99

up to more than 10wt% in DF1 in the presence of about 10wt% ZnO and 6wt% Na_2O the fluidity of glaze is intensified and much recrystallization of the (Na_2O, ZnO)-zirconium, alumino silicate s.s. occurs on cooling at the expense of zircon and plagioclase s.s. Additionally, the longer firing/cooling schedule used for double-fired glaze (DF1) has increased the rate of crystallization of the (Na_2O, ZnO)-zirconium alumino silicate s.s. as compared with that of the once-fired sample (OF1). In the latter glaze, this phase could not easily be detected by XRD (Fig. 4); it seems to be in the amorphous state as detected by EPMA. The point analysis (Table 4) shows that the amorphous phase in OF1 contains higher amounts of SiO_2 and ZrO_2 and lower amounts of Na_2O, ZnO and Al_2O_3 than that of DF1 glaze.

In glaze OF1, a zircon-rich mat layer having a thickness of about 30 μm is shown at the surface of very bright glaze bulk. This layer exhibits relatively low ZnO and high ZrO_2 and SiO_2 contents than the glaze bulk. The seggregation of this glaze into two distinct layers may be a result of insufficient deflocculation of its glaze slip and/or the lower content of B_2O_3(4·18wt%). This may be also due to the loss of B_2O_3 by evaporation through the surface as detected in Fig. 1 for DF1 glaze as an example.

Table 5 illustrates the physical properties of the glazed tile samples. It is evident that once-fired glazes have generally higher melting temperatures than those of double-fired ones. This is mainly attributed to the higher Al_2O_3 and ZrO_2 contents of the former glazes. The relative lower melting temperatures of DF3 and OF3 glazes in comparison with their corresponding samples are probably due to the combination of comparable amounts of K_2O and Na_2O. This leads to lowering the eutectic temperature of the whole glaze oxide batches.[3,4]

The results of glaze-surface gloss indicate that double-fired samples show generally better gloss values (87–95) than the once-fired (16–88). In double-fired glazes, the decrease of gloss in DF2 can be attributed to its lower ZnO content (1·9wt%) as compared with DF1 (10·0wt%) and DF3 (5·3wt%). On the other hand, the great deterioration of gloss of glaze OF1 is due to the formation of a seggregated mat layer at its surface as shown previously in Fig. 2. This figure also exhibits an unsmooth surface for OF2 and OF3 glazes due to the formation of numerous pin-holes in the former and some pits in the latter. Therefore, the gloss of these glazes is reduced to 58 and 88, respectively.

The calculated thermal expansion coefficients of ceramic body and glaze samples measured between 20 and 580°C are also summarized in Table 5. The temperature of 580°C is selected from the thermal expansion curves of the glazes made up to about 650°C because it exists within the temperature range including the lower critical temperature (T), at which the rate of expansion begins to increase rapidly. At this temperature, the difference in expansion between body and glaze determines the stress set in the cold glazed tiles.

From Table 5 it is evident that double-fired glazes show generally higher thermal expansions than once-fired samples due to the longer firing/cooling cycle of the former type (18 h).[15] Glazes DF1 and OF1, which have more crystalline silicate phases, show higher thermal expansion than the other double- and once-fired samples, respectively. The latter samples contain only zircon as crystalline a phase. Both of the double- and once-fired glazes show slightly lower expansion than the ceramic body in its fired and green state (Table 5). In such a case, the final glaze stress is compressive and satisfactory fitness between glaze and body is expected.[3,4] This is confirmed by the

Table 5. Physical properties of double- and once-fired glaze samples

	Double-fired glaze				Once-fired glaze			
	DF1	DF2	DF3	body	OF1	OF2	OF3	body
Melting temp. (°C)	940	940	920	—	1020–1040	1020	1000–1020	—
Average gloss (60°C)	95	87	91	—	16	58	88	—
Thermal expansion coefficient × 10^{-6}	6·1	5·3	5·6	6·4	5·8	4·9	5·1	6·2

high crazing resistance of all the glazed tile samples. No evidence of crazing was observed under vapour pressure, even after soaking identical uncut tile samples for 5 h up to 250 psi. The higher crazing resistance of the studied samples can also be related to the interaction layer between glaze and body, which has intermediate chemical composition.[16] Furthermore, the presence of 3·0–6·0wt% of K_2O and/or Na_2O in the studied glazes leads to the development of the tetra-coordinated boron which is bonded more strongly in the glaze vitreous matrix than the normal tri-coordinated one.[17]

4 CONCLUSIONS

1. The formation of a proper interaction layer having intermediate chemical composition and physical properties between glaze and ceramic body leads to the high crazing resistance of glaze surfaces.

2. The application of zircon-ZnO opacifying mixtures with the addition of 5·0–8·0wt% B_2O_3 is helpful in maximizing the gloss of glaze surfaces.

3. The recrystallization of silicate phases, especially in double-fired glazes, is hindered by minimizing lime and alkali oxides contents in the presence of up to 10wt% ZnO.

ACKNOWLEDGEMENTS

The authors are greatly indebted to the Ministry of Science and Art/Stuttgart, to the German Academic Exchange Organization (DAAD)/Bonn and to the International Seminar/University of Karlsruhe, Federal Republic of Germany for the financial support and facilities provided to conduct this work. Thanks are also extended to Mr. H. Herberger, Institute of Chemical Technology/University of Karlsruhe for preparing the investigated samples for microanalysis.

REFERENCES

1. RUDDLESDEN, S. N., Applications of the electron probe microanalyzer to ceramics. Parts I-III. *Trans. Brit. Ceram. Soc.*, **66** (1967) 587–629.
2. RUDDLESDEN, S. N., The application of electron probe microanalysis to textural studies of ceramics. *Proc. Brit. Ceram. Soc.*, **20** (1972) 1–25.
3. PARMALEE, C. W., *Ceramic Glazes*. Cahners Books, Boston, 1973.
4. SHAW, K., *Ceramic Glazes*. Elsevier Science, Amsterdam, Oxford, New York, 1971.
5. DIETZEL, A. & KESTAN, W., Reaction between body and glaze and its relation to the problem of crazing. *Berichte Deutsche Keram. Ges.*, **31** (1954) 320.
6. SAINZ, I. G., Physical-chemical characteristics of ceramic glazes and their influence on quality of floor and wall tiles. *Tile Brick Int.*, **6**(6) (1990) 21.
7. EL-DEFRAWI, S. A. & ABD EL-FATTAH, W. I., Pinholes and introduction of albite in double firing zircon-glazed tiles. *Silicates Industriels*, **58**(1–2) (1993) 31.
8. ABD EL-FATTAH, W. I. & EL-DEFRAWI, S. A., Diagnosis and remedy of pinholes in monoporosa wall tiles. *Bull. Fac. Sc. Zagazig Univ.*, **16**(2) (1994) a39–54.
9. WILLIAMSON. W. O., Bubbles and associated structures in fired glazes: hypotheses and microscopical observations. *Trans. Brit. Ceram. Soc.*, **59** (1960) 455.
10. APARICL, J. & MARENO, A., Porosity in single firing glazes for floor tiles. *Tile Brick Int.*, **6**(6) (1990) 33.
11. PICARD, W. G., BACHERE, S. T. & HOFFMANN, D. W., Leadless fast-fired glazes. *Interceram.*, **36**(3) (1987) 36.
12. BRIDGER, K. E., The glazing of fast once-fired tiles. *Interceram.*, **34**(3) (1985) 15.
13. NORRIS, A. W., Some physical properties of glazes. *Trans. Brit. Ceram. Soc.*, **55**(10) (1956) 601.
14. JACOBS, W. F., Opacifying crystalline phases present in zirconium-type glazes. *J. Am. Ceram. Soc.*, **37**(5) (1954) 216.
15. BULL, A. C., Bodies, glazes and colours for fast firing. Review Paper given at Meeting of the Brit. Ceram. Soc., Stoke-On-Trent, 1981.
16. INADA, H., Effect of the glaze–body reaction on the fitness of glaze and body of chinaware. *Interceram.*, **18**(3) (1979) 310.
17. FERROM, R., FURLONI, C. HREGLICH, S. & LOCADI, B., X-ray microanalytical electron-spectroscopic ESCA and optical microscopic study of changes at interface of enameled tiles due to firing and their effect on crazing phenomenon. *Ceram. Inf.*, **21** (1986) 77–83.